Centrality and transverse momentum dependence of hadrons in Pb+Pb collisions at LHC

Lilin Zhu,[1,*] Hua Zheng,[2,†] and Rudolph C. Hwa[3,‡]

[1] *Department of Physics, Sichuan University, Chengdu 610064, China*
[2] *School of Physics and Information Technology, Shaanxi Normal University, Xi'an 710119, China*
[3] *Institute of Theoretical Science and Department of Physics, University of Oregon, Eugene, OR 97403-5203, USA*

The transverse momentum spectra of seven identified hadrons produced in Pb+Pb collisions at $\sqrt{s_{NN}} = 2.76$ and 5.02 TeV at the CERN Large Hadron Collider (LHC) have been investigated in the framework of the recombination model (RM). The investigation has been extended to non-central collisions and the parameters controlling the momentum degradation of semihard partons have been tuned. Results from RM calculations are compared with the available experimental data. Good agreements are generally found between theoretical results and experimental data, except that the proton and Ξ spectra at peripheral collisions underestimate the data at very low p_T. Possible reason for the discrepancy is discussed. The transverse momentum spectra of Λ, ϕ, Ξ and Ω at various centralities in Pb+Pb collisions at $\sqrt{s_{NN}} = 5.02$ TeV are predicted for the future experimental data test.

PACS numbers: 25.75.Nq, 25.75.Ld

I. INTRODUCTION

The ultimate goal of the physics program with ultrarelativistic nucleus-nucleus collisions is to study the properties of strongly interacting matter under extreme conditions of high temperature and density. Quantum Chromodynamics (QCD) predicts that strongly interacting matter undergoes a phase transition from a state of hadronic constituents to quark and gluon plasma (QGP). One of the most promising signals of the deconfinement is related to particular properties of transverse momentum spectra of final hadrons. The conventional method for hadron production in heavy-ion collisions is hydrodynamical description for transverse momentum $p_T < 3$ GeV/c [1–3] and jet fragmentation for the region of $p_T > 8$ GeV/c [4–6]. In the intermediate region both approaches are not applicable, while the recombination or coalescence (ReCo) model in heavy-ion collisions has been found to be more relevant [7–9]. The large baryon-to-meson ratio is a signature of ReCo, which has shown some success in filling the gap [7–11].

Despite differences in detail, the basic ideas of the three formulations of ReCo are very similar [7–9]. In this study, Hwa-Yang recombination model (RM) is adopted [7]. It is formulated in one dimension on the foundation that noncollinear partons have low probability of coalescence, and has incorporated fragmentation as a component of recombination so that there is a smooth transition from low to high p_T. Within the framework of RM, the transverse momentum and centrality dependence of hadrons production in Au+Au collision at $\sqrt{s_{NN}} = 200$ GeV at RHIC were well reproduced [10]. It is found that the recombination of thermal and shower partons is the major component for intermediate p_T region. In heavy-ion collisions above 2 TeV, the density of minijets produced by semihard scatterings of partons can be so high that the conventional treatment of such collisions may be inadequate. Recently, the spectra of hadrons produced in central Pb+Pb collisions at $\sqrt{s_{NN}} = 2.76$ TeV has been studied with p_T up to 20 GeV/c by the recombination model [11]. It is found that there is an abundance of minijet produced at $\sqrt{s_{NN}} = 2.76$ TeV. These previous studies [10, 11] have revealed that the formation of hadrons at intermediate p_T region is sensitive to the momentum degradation of the hard and semihard partons. Furthermore, due to the geometrical configuration of colliding system, the momentum degradation from the initial parton momentum to the final momentum at the medium surface is different for Au+Au and Pb+Pb collisions. Even for the same colliding system, the momentum degradation is not the same for different colliding energies. We will give more discussion later.

In heavy-ion collisions there are various theoretical issues related to minijets that have not yet evolved to a mature subject with general acceptance. The medium effects on semihard partons are important but hard to make precise, and the hadronization process is still controversial. The shower partons not only depend on the momentum degradation in the medium, but also can be hadronized through various channels, such as recombination with thermal partons on the one hand and with other shower partons on the other. At LHC the high density of jets enables the possibility of shower partons from different jets overlapping in common spatial proximity so that the contribution from their coalescence cannot be ignored. Although we have studied the minijet contribution to the central Pb+Pb collisions at $\sqrt{s_{NN}} = 2.76$ TeV, it is not conclusive from the observed p_T spectra

*Electronic address: zhulilin@scu.edu.cn
†Electronic address: zhengh@snnu.edu.cn
‡Electronic address: hwa@uoregon.edu

that minijets are necessarily existent. Therefore, we will extend the investigation of the p_T spectra of identified hadrons to non-central collisions in Pb+Pb collisions at both $\sqrt{s_{NN}} = 2.76$ and 5.02 TeV with the recombination model in this study and try to draw a conclusion for the hadronization mechanism in nuclear collisions.

The paper is organized as follows: In Section II, we briefly review the basic framework of Hwa-Yang recombination model, including the inclusive distribution of minijets. The formalisms of parton combination for pion, proton and kaon are shown in Section III. In Section IV, we show results from our study on the centrality dependence of transverse momentum spectra of seven identified hadrons in Pb+Pb collisions at $\sqrt{s_{NN}} = 2.76$ and 5.02 TeV. Finally, section V summarizes the results and gives the conclusion from the present study.

II. BASIC FRAMEWORK OF RECOMBINATION MODEL

Let us start by recalling the basic elements of the recombination model. Our study here is limited to the midrapidity and all the formulae are averaged over the azimuthal angles. Therefore, the invariant distributions of mesons and baryons are, which are averaged over η at midrapidity [7, 10, 11, 24, 25]

$$p^0\frac{dN^M}{dp_T} = \int \frac{dp_1}{p_1}\frac{dp_2}{p_2}F_{q_1\bar{q}_2}(p_1,p_2)R^M_{q_1\bar{q}_2}(p_1,p_2,p_T), \quad (1)$$

$$p^0\frac{dN^B}{dp_T} = \int \frac{dp_1}{p_1}\frac{dp_2}{p_2}\frac{dp_3}{p_3}F_{q_1q_2q_3}(p_1,p_2,p_3) \times R^B_{q_1q_2q_3}(p_1,p_2,p_3,p_T), \quad (2)$$

with the transverse momenta of coalescing quarks p_i. R^M and R^B are the recombination functions (RFs) of the corresponding quarks for mesons and baryons, respectively. The parton distributions can be partitioned into various components, represented symbolically by

$$F_{q_1\bar{q}_2} = \mathcal{TT} + \mathcal{TS} + \mathcal{SS}, \quad (3)$$

$$F_{q_1q_2q_3} = \mathcal{TTT} + \mathcal{TTS} + \mathcal{TSS} + \mathcal{SSS}, \quad (4)$$

where $\mathcal{T}$ and $\mathcal{S}$ represent the invariant distributions for thermal and shower partons just before hadronization, respectively. The former contains the medium effect, while the latter is due to semihard and hard scattered partons. The consideration of shower partons is a unique feature of our model to recombination, which is empowered by the possibility to include fragmentation process as $\mathcal{SS}^{1j}$ or $\mathcal{SSS}^{1j}$ recombination. For the contribution with two or three shower partons, we need to take into account their sources. As becomes self-evident, the theoretical description that includes all components of hadronization (4 components for mesons and 7 components for baryons) is sufficiently complicated. For the visualization of the various processes, we refer to the schematic diagrams in Ref. [11]. The shower partons in $\mathcal{SS}$ and $\mathcal{TSS}$ can be from the same jet or two jets. For $\mathcal{SSS}$, only the contributions of $\mathcal{SSS}^{1j}$ and $\mathcal{SSS}^{2j}$ are included in this study, because the contribution of the $\mathcal{SSS}^{3j}$ referring to that the three shower partons are from three jets is highly suppressed.

$\sqrt{s}$ (TeV)	2.76	5.02
T_q (GeV)	0.39	0.415
T_s (GeV)	0.51	0.545

TABLE I: Parameters T_q and T_s for Pb+Pb collisions at $\sqrt{s} =$ 2.76 and 5.02 TeV, respectively.

The thermal parton distribution is assumed to have a simple exponential form

$$\mathcal{T}_j(p_i) = p_i\frac{dN_j}{dp_i} = C_j p_i e^{-p_i/T_j}, \quad (5)$$

where the subscript j denotes light quark (u, d, s). Since the mass of s is different from (u, d), to distinguish them, we use q denotes (u, d). The normalization factor C_j has the dimension of inverse momentum. The inverse slope T_j is treated as a parameter to be determined by fitting the experimental data of spectra at low p_T. It includes the dissipative effects of minijets on the expanding medium at all times of the plasma evolution. A universal formula for the energy dependence of T_j was obtained in [27],

$$T_q(s) = T_1 f(s), \qquad T_s(s) = T_2 f(s), \quad (6)$$

$$f(s) = \sqrt{s}^{\,\beta}, \qquad \sqrt{s} \text{ in TeV}, \quad (7)$$

with the parameters

$$T_1 = 0.35 \text{ GeV/c}, \quad T_2 = 0.46 \text{ GeV/c}, \quad \beta = 0.105. \quad (8)$$

For simplicity, we have used $\sqrt{s}$ to replace $\sqrt{s_{NN}}$. The values of T_j for $\sqrt{s} = 2.76$ and 5.02 TeV are given in Table I.

As discussed in Ref. [11], the shower parton distribution is given by

$$\mathcal{S}^j(p_2) = \int \frac{dq}{q}\sum_i \hat{F}_i(q)S^j_i(p_2,q), \quad (9)$$

where $S^j_i(p_2, q)$ is the shower parton distribution (SPD) in a jet of type i fragmentating into a parton of type j with momentum fraction of p_2/q. It is determined by the fragmentation functions (FFs) known from analyzing leptonic processes on the basis that hadrons in a jet are formed by recombination of the shower partons in the jet [26]. The SPD does depend strongly on the collision energy due to the increased rate of creation of hard partons and the quenching effect of the denser medium. Once the SPDs are known, one can give a more complete

description of hadronization, especially for the nuclear collisions. After including the centrality dependence, Eq. (9) should be modified as

$$\mathcal{S}^j(p_2,c) = \int \frac{dq}{q} \sum_i \hat{F}_i(q,c) S_i^j(p_2,q). \tag{10}$$

$\hat{F}_i(q,c)$ is the distribution of hard and semihard parton of type i at the medium surface after momentum degradation while transversing the medium. At a specified centrality c, e.g. $c = 0.05$ stands for $0-10\%$ centrality, it is defined as

$$\begin{aligned}\hat{F}_i(q,c) &= \frac{1}{2\pi}\int d\phi \int d\xi P_i(\xi,\phi,c) \\ &\times \int dk k f_i(k,c) G(k,q,\xi),\end{aligned} \tag{11}$$

$P_i(\xi,\phi,c)$ is the probability for the parton i having a dynamical path length ξ at angle ϕ initiated at position (x_0,y_0), weighted by the nuclear overlap function and integrated over all (x_0,y_0). The connection between geometry and dynamics is imbedded in $P_i(\xi,\phi,c)$. The dynamical path length ξ is proportional to the geometrical path length l. Therefore, $P_i(\xi,\phi,c)$ can be written as

$$P_i(\xi,\phi,c) = \int dx_0 dy_0 Q(x_0,y_0,c)\delta(\xi - \gamma_i l). \tag{12}$$

where $Q(x_0,y_0,c)$ is the probability that a hard (or semihard) parton is produced at (x_0,y_0), which can be calculated from nucleon thickness functions [10]. The factor γ_i is introduced to account for the effects of jet quenching in the medium that results in additional parton degradation due to the soft partons created. We will discuss this factor in details later.

The function $f_i(k,c)$ is the density of parton i in the phase space kdk. For central collisions, the initial momentum distribution $f_i(k,c)$ was parametrized as [28]

$$f_i(k,0.05) = K\frac{A}{(1+k/B)^\beta}. \tag{13}$$

For Pb+Pb collisions at 2.76 TeV, the parameters in Eq. (13) were obtained by logarithmic interpolations of the parameters $\ln A$, B and β between Au+Au collisions at 200 GeV and Pb+Pb collisions at 5.5 TeV with $K = 2.5$, as shown in Ref. [11]. Following the same approach, we can get the parameters for central Pb+Pb collisions at 5.02 TeV listed in TABLE II. Taking into account the centrality dependence, the minijet distribution can be calculated by

$$f_i(k,c) = \frac{T_{AA}(c)}{T_{AA}(0.05)} f_i(k,0.05). \tag{14}$$

The nuclear thickness function $T_{AA}(c)$ for Pb+Pb collisions are available in Ref. [23].

For the momentum degradation function $G(k,q,\xi)$ due to energy loss, as discussed before [11], we take the simple form

$$G(k,q,\xi) = q\delta(q - ke^{-\xi}) \tag{15}$$

as an adequate approximation of the complicated processes involved in the parton medium interaction.

Therefore, $\hat{F}_i(q,c)$ can be calculated once γ_i is fixed. Unfortunately, we cannot calculate γ_i directly, since the effect of energy loss during the passage of the parton through the non-uniform and expanding medium is not clear. Considering the quark and gluon lose their energies at different rates when they go through the medium, we assumed that $\gamma_q = \gamma_g/2 = 0.07$ and obtained excellent fits for hadron spectra in Au+Au collisions at $\sqrt{s_{NN}} = 200$ GeV [10] . For the momentum degradation at LHC, the γ_i factor could not remain the same as that at RHIC due to many more minijets produced and the different geometrical configuration of colliding system. For Pb+Pb collisions, we parametrized it as [11]

$$\gamma_g(q) = \frac{\gamma_0}{1+(q/q_0)^2}. \tag{16}$$

The parameters γ_0 and q_0 are determined by fitting the spectra in the intermediate p_T region. For Pb+Pb collisions at 2.76 TeV, we have obtained $\gamma_0 = 2.8$ and $q_0 = 7$ GeV/c [11]. Their values for Pb+Pb collisions at 5.02 TeV will be discussed in Sec. IV.

III. INCLUSIVE DISTRIBUTIONS OF HADRONS

After the semihard parton distributions $\hat{F}(q,c)$ for all species and any centrality are obtained, we can be more explicit about hadron formation by recombination. The formulae for recombination of thermal and shower partons at central collisions have been developed previously [11]. We generalize them for pion, kaon, and proton production to non-central collisions here. The centrality dependence of other mesons and hyperons production can be derived in similar way.

A. Pion production

The RF for pion is given in Refs. [7, 10, 11, 24, 25]

$$R^\pi(p_1,p_2,p_T) = \frac{p_1 p_2}{p_T}\delta(p_1+p_2-p_T). \tag{17}$$

	g	u	d	$\bar{u}$	$\bar{d}$	s, $\bar{s}$
A [10^4/GeV^2]	11.2	2.02	2.28	0.42	0.40	0.154
B [GeV]	0.80	0.59	0.58	0.75	0.76	0.93
β	5.68	5.31	5.29	5.52	5.53	5.63

TABLE II: Parameters for $f_i(k, 0.05)$ in Eq. (13) for central Pb+Pb collisions at $\sqrt{s} = 5.02$ TeV.

Following Eqs. (1), (3) and (17), the four components for pion production are

$$\frac{dN_\pi^{TT}}{p_T dp_T} = [1 + u(p_T, N_{part})]\frac{C^2}{6}e^{-p_T/T}, \quad (18)$$

$$\frac{dN_\pi^{TS}}{p_T dp_T} = \frac{C}{p_T^3}\int_0^{p_T} dp_1 p_1 e^{-p_1/T} \times \left[\mathcal{S}^u(p_T - p_1, c) + \mathcal{S}^{\bar{d}}(p_T - p_1, c)\right], \quad (19)$$

$$\frac{dN_\pi^{SS^{1j}}}{p_T dp_T} = \frac{1}{p_T}\int \frac{dq}{q^2}\sum_i \hat{F}_i(q, c) D_i^\pi(p_T, q), \quad (20)$$

$$\frac{dN_\pi^{SS^{2j}}}{p_T dp_T} = \frac{\Gamma}{p_T^3}\int_0^{p_T} dp_1 \mathcal{S}^u(p_1, c)\mathcal{S}^{\bar{d}}(p_T - p_1, c). \quad (21)$$

The extra factor $u(p_T, N_{part})$ in Eq. (18) is due to the contribution from the resonance decays, which dominates for pion distribution at $p_T < 2$ GeV/c. The shower-shower recombination from one jet (SS^{1j}) is equivalent to fragmentation, so we can use the FFs D_i^π directly in Eq. (20). Γ in Eq. (21) is the probability that two parallel partons originated from two jets can recombine. As done in Ref. [11], Γ was estimated as the ratio of pion diameter to nuclear diameter, which is about 0.1.

B. Proton production

Compared with pion, proton mass is not negligible. p^0 in Eq. (3) should be replaced by the transverse mass $m_T^p = \sqrt{p_T^2 + m_p^2}$. The RF for protons is given in Refs. [7, 10, 11, 24, 25], which includes the momentum conservation δ function. The thermal-thermal-thermal (TTT) recombination is

$$\frac{dN_p^{TTT}}{p_T dp_T} = g_{st}^p g_p g_p' \frac{C^3 p_T^2}{m_T^p} e^{-p_T/T}, \quad (22)$$

where $g_{st}^p = 1/6$ and

$$g_p = [B(\alpha + 1, \alpha + \beta + 2)B(\alpha + 1, \beta + 1)]^{-1}, \quad (23)$$

$$g_p' = B(\alpha + 2, \beta + 2)B(\alpha + 2, \alpha + \beta + 4). \quad (24)$$

$B(\alpha, \beta)$ is the beta function with $\alpha = 1.75$ and $\beta = 1.05$.

For thermal-thermal-shower (TTS), thermal-shower-shower (TSS) and shower-shower-shower (SSS) recombination, we have

$$\frac{dN_p^{TTS}}{p_T dp_T} = \frac{g_{st}^p g_p C^2}{m_T^p p_T^{2\alpha+\beta+3}}\int_0^{p_T} dp_1 \int_0^{p_T - p_1} dp_2\, e^{-(p_1+p_2)/T}\left\{(p_1 p_2)^{\alpha+1}(p_T - p_1 - p_2)^\beta \mathcal{S}^d(p_T - p_1 - p_2, c) + p_1^{\alpha+1} p_2^{\beta+1}(p_T - p_1 - p_2)^\alpha \mathcal{S}^u(p_T - p_1 - p_2, c)\right\}, \quad (25)$$

$$\frac{dN_p^{TSS^{1j}}}{p_T dp_T} = \frac{g_{st}^p g_p C}{m_T^p p_T^{2\alpha+\beta+3}}\int_0^{p_T} dp_1 \int_0^{p_T - p_1} dp_2\, e^{-p_1/T}\left\{p_1^{\beta+1} p_2^\alpha (p_T - p_1 - p_2)^\alpha \mathcal{S}^{uu}(p_2, p_T - p_1 - p_2, c) + p_1 (p_1 p_2)^\alpha (p_T - p_1 - p_2)^\beta \mathcal{S}^{ud}(p_2, p_T - p_1 - p_2, c)\right\}, \quad (26)$$

$$\frac{dN_p^{TSS^{2j}}}{p_T dp_T} = \frac{g_{st}^p g_p C\Gamma}{m_T^p p_T^{2\alpha+\beta+3}}\int_0^{p_T} dp_1 \int_0^{p_T - p_1} dp_2\, e^{-p_1/T}\left\{p_1^{\beta+1} p_2^\alpha (p_T - p_1 - p_2)^\alpha \mathcal{S}^u(p_2, c)\mathcal{S}^u(p_T - p_1 - p_2, c) + p_1 (p_1 p_2)^\alpha (p_T - p_1 - p_2)^\beta \mathcal{S}^u(p_2, c)\mathcal{S}^d(p_T - p_1 - p_2, c)\right\}, \quad (27)$$

$$\frac{dN_p^{SSS^{1j}}}{p_T dp_T} = \frac{1}{m_T^p}\int \frac{dq}{q^2}\sum_i \hat{F}_i(q, c) D_i^p(p_T, q), \quad (28)$$

$$\frac{dN_p^{SSS^{2j}}}{p_T dp_T} = \frac{g_{st}^p g_p \Gamma}{m_T^p p_T^{2\alpha+\beta+3}} \int_0^{p_T} dp_1 \int_0^{p_T-p_1} dp_2 \left\{ p_1^\beta p_2^\alpha (p_T - p_1 - p_2)^\alpha \mathcal{S}^d(p_1, c) \mathcal{S}^{uu}(p_2, p_T - p_1 - p_2, c) + (p_1 p_2)^\alpha (p_T - p_1 - p_2)^\beta \mathcal{S}^u(p_1, c) \mathcal{S}^{ud}(p_2, p_T - p_1 - p_2, c) \right\}, \quad (29)$$

where

$$\mathcal{S}^{qq}(p_2, p_3, c) = \int \frac{dq}{q} \sum_i \hat{F}_i(q, c) \mathrm{S}_i^q(p_2, q) \mathrm{S}_i^q(p_3, q - p_2). \quad (30)$$

C. Kaon production

The four components of kaon distribution are very similar to those of pion. The differences are in the constituent quark masses between m_q and m_s resulting in asymmetry of the RF for kaon and the different T_q of light quarks and T_s of s quarks. The kaon production is written as

$$\frac{dN_K^{TT}}{p_T dp_T} = \frac{12 C C_s}{m_T^K p_T^5} \int_0^{p_T} dp_1 p_1 (p_T - p_1)^2 \times p_1 e^{-p_1/T} (p_T - p_1) e^{-(p_T - p_1)/T_s}, \quad (31)$$

$$\frac{dN_K^{TS}}{p_T dp_T} = \frac{12}{m_T^K p_T^5} \int_0^{p_T} dp_1 p_1^2 (p_T - p_1)^2 \left[C e^{-p_1/T} \mathcal{S}^{\bar{s}}(p_T - p_1, c) + C_s \left(\frac{p_T}{p_1} - 1 \right) e^{-(p_T - p_1)/T_s} \mathcal{S}^u(p_1, c) \right], \quad (32)$$

$$\frac{dN_K^{SS^{1j}}}{p_T dp_T} = \frac{1}{m_T^K} \int \frac{dq}{q^2} \sum_i \hat{F}_i(q, c) D_i^K(p_T, q), \quad (33)$$

$$\frac{dN_K^{SS^{2j}}}{p_T dp_T} = \frac{12\Gamma}{m_T^K p_T^5} \int_0^{p_T} dp_1 p_1 (p_T - p_1)^2 \times \mathcal{S}^u(p_1, c) \mathcal{S}^{\bar{s}}(p_T - p_1, c). \quad (34)$$

IV. RESULTS

So far, we have treated the momentum degradation of minijets and determined the distribution of semi-hard parton $\hat{F}_i(q, c)$ for any centrality and the formalism for hadronization in Secs. II and III, respectively. The hadron production in central Pb+Pb collisions at $\sqrt{s_{NN}} = 2.76$ TeV has been studied in our earlier work [11]. In this work, we extend the investigation to non-central collisions in Pb+Pb collisions at both $\sqrt{s_{NN}} = 2.76$ and 5.02 TeV in the same framework. We emphasize

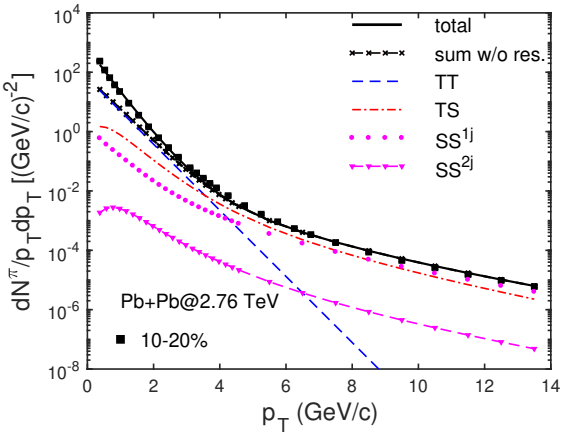

FIG. 1: (Color online) Transverse momentum spectrum of pion at the centrality of 10-20% in Pb+Pb collisions at $\sqrt{s_{NN}} = 2.76$ TeV. The data are from Ref. [29].

that there is no parameter to adjust for the intermediate and high p_T regions, since all details on minijets have been specified in Sec. II. For thermal partons, the inverse slopes T and T_s are independent of centrality [27], so the unknown parameters are just the centrality dependence of normalization factors, C and C_s.

The transverse momentum spectra of pion and proton in Pb+Pb collisions at $\sqrt{s_{NN}} = 2.76$ TeV and centrality of 10-20% are shown in Figs. 1 and 2, respectively. The data are taken from the ALICE collaborations [29]. The thermal and shower components in various combinations are shown by different line types. The blue dashed lines show the TT and TTT components, whose magnitudes are determined by fitting the experimental data. What one can see is that the pion distribution without the resonance contribution is lower than the data for $p_T < 2$ GeV/c in Fig. 1. Therefore, the extra term $u(p_T, N_{part})$ is inserted in Eq. (18) for pions,

$$u(p_T, N_{part}) = (2.8 + 0.003 N_{part}) e^{-p_T/0.45}, \quad (35)$$

where N_{part} is the number of participants. After taking into account the contribution from resonance decays, the solid line can reproduce the pion distribution for the whole p_T region very well. In Fig. 2, the proton dis-

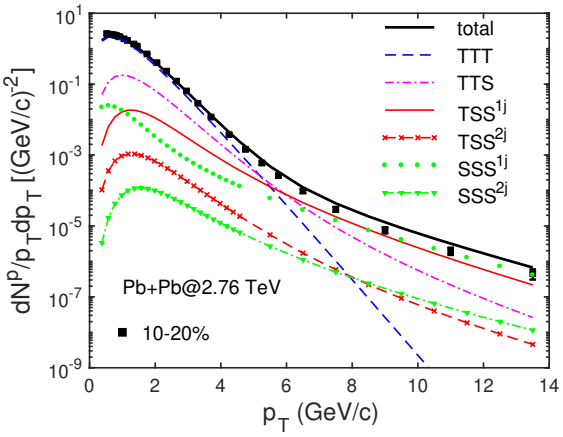

FIG. 2: (Color online) Transverse momentum spectrum of proton at the centrality of 10-20% in Pb+Pb collisions at $\sqrt{s_{NN}} = 2.76$ TeV. The data are from Ref. [29].

tribution is nicely reproduced as well. Compared with the various components of pion and proton for central collisions in Ref. [11], one can see that the results are very similar. The thermal and shower recombination is tremendously important for the hadron production at intermediate p_T region. Then we can continue to study the strange hadron spectra, i.e., K, Λ, ϕ, Ξ and Ω. The explicit formulae for the various components of Λ, Ξ, Ω and ϕ are shown in Appendix A-D of Ref. [11].

Figure 3 shows the transverse momentum spectra of seven identified hadrons, i.e.,π, p, K, Λ, ϕ, Ξ and Ω, from RM in Pb+Pb collisions at $\sqrt{s_{NN}} = 2.76$ TeV and 0-5%, 10-20%, 20-40% and 40-60% centralities. The distributions for the centrality of 0-5% are taken from our earlier work [11]. Similar to Fig. 1, the spectra of pion nicely describe the ALICE data for the whole p_T region for the other three centralities by adjusting the normalization factor C, whose values for various centralities are listed in TABLE III. Without changing any parameter we calculate the proton distributions shown in Fig. 3(b). The results from central to less central collisions agree with the experimental data well. For centrality 40-60%, the calculation is a little bit lower than the data at very low p_T. At peripheral collisions, the nuclear overlap is a very narrow almond-shaped region. At the two tips of the almond, the collisions are essentially similar to pp collisions. Even along the boundary of the nuclear overlap, the nuclear thickness is thin. The thin layer along the boundary of the almond involves pA' collisions, where A' is smaller than A. Those collisions are not likely to be thermalized by the bulk in the interior. In this sense, a significant part of protons detected at low p_T in peripheral collisions belong to the remainder that is associated with the proton projectile due to the border region of the nuclear overlap, since the border region becomes a significant portion of the whole overlap. It is non-thermal. In other words, a non-thermal component at low p_T region needs to be considered for peripheral collisions, which is submerged below the dominant contribution in the central collisions. The investigation about this is out of the scope of this work.

For the production of kaons, the inverse slope T_s is determined by Eqs. (6)-(8) and shown in TBALE I. Hence, C_s is the only one adjustable parameter to fit the data. Its values for the centralities of 0-5%, 10-20%, 20-40% and 40-60% are established in TABLE III. As shown in Fig. 3(c), the data for kaons at four centralities are well reproduced. For the other strange particles ϕ, Λ, Ξ and Ω, we use the same C_s and T_s from kaons. Without any parameter to adjust, the calculations from RM can describe the experimental data of Λ, ϕ and Ω at four centralities very well in Fig. 3(d), (e) and (g). For Ξ in Fig. 3(f), the spectrum at 0-5% can be nicely reproduced, while for non-central collisions the calculations from RM underestimate the measured data at low p_T. This is similar to proton. It may be due to the non-thermal component contribution as well. [This is our speculation for Ξ. We are not sure about it.]

The excellent results shown in Fig. 3 corroborate that recombination model still works for non-central collisions in Pb+Pb collisions at $\sqrt{s_{NN}} = 2.76$ TeV and this encourages us to study the hadron production for higher colliding energy $\sqrt{s_{NN}} = 5.02$ TeV. Due to the higher colliding energy, the dynamical effect of energy loss is stronger. Therefore, the parameter γ_i for parton degradation at 5.02 TeV should be different from that for 2.76 TeV. Before determining the γ_i factor for $\sqrt{s_{NN}} = 5.02$ TeV, let us first look at the nuclear modification factor R_{AA} for charged particles in Pb+Pb collisions measured at $\sqrt{s_{NN}} = 2.76$ TeV and 5.02 TeV [34]. R_{AA} has a strong centrality dependence and is very similar in magnitude for the two collision energies. In 0-5% central collisions the yield is suppressed by a factor of about 8 ($R_{AA} \sim 0.13$) at $p_T = 6 \sim 7$ GeV/c. Above $p_T = 7$ GeV/c, there is a significant rise of the nuclear modification factor, which reaches a value of about 0.4 around $p_T = 40$ GeV/c. The similar behavior can be found for the other centralities. In this sense, we still choose $q_0 = 7$ GeV/c for $\sqrt{s_{NN}} = 5.02$ TeV. To fit the spectra of pion and proton for intermediate p_T at central collisions, we use $\gamma_0 = 4.5$. Figure 4 shows the transverse momentum spectra of π, p, K, Λ, ϕ, Ξ and Ω in Pb+Pb collisions at $\sqrt{s_{NN}} = 5.02$ TeV. The normalization factors C and C_s for various centralities are given in TABLE III. The spectra of π and K nicely describe the ALICE data for p_T up to 14 GeV/c in Pb+Pb collisions at $\sqrt{s_{NN}} = 5.02$ TeV for the centralities of 0-5%, 30-40% and 60-70%. Similar to $\sqrt{s_{NN}} = 2.76$ TeV, for protons, there is still a small deviation between the calculation and data for very low p_T region at 60-70%. With the retuned parameters C and C_s, we predict the spectra of Λ, ϕ, Ξ and Ω in central and non-central Pb+Pb collisions at $\sqrt{s_{NN}} = 5.02$ TeV with recombination model, which can be tested when the experimental data are published in future.

In an overall view of Figs. 3 and 4, it is remarkable that

$\sqrt{s}$ [TeV]	centrality	C [(GeV/c)$^{-1}$]	C_s [(GeV/c)$^{-1}$]
2.76	0-5%	23.2	11.0
	10-20%	19.5	9.2
	20-40%	15.5	7.33
	40-60%	11.0	5.04
5.02	0-5%	22.0	10.0
	30-40%	13.4	6.55
	60-70%	6.8	3.40

TABLE III: Parameters C and C_s for Pb+Pb collisions at $\sqrt{s} = 2.76$ and 5.02 TeV, respectively.

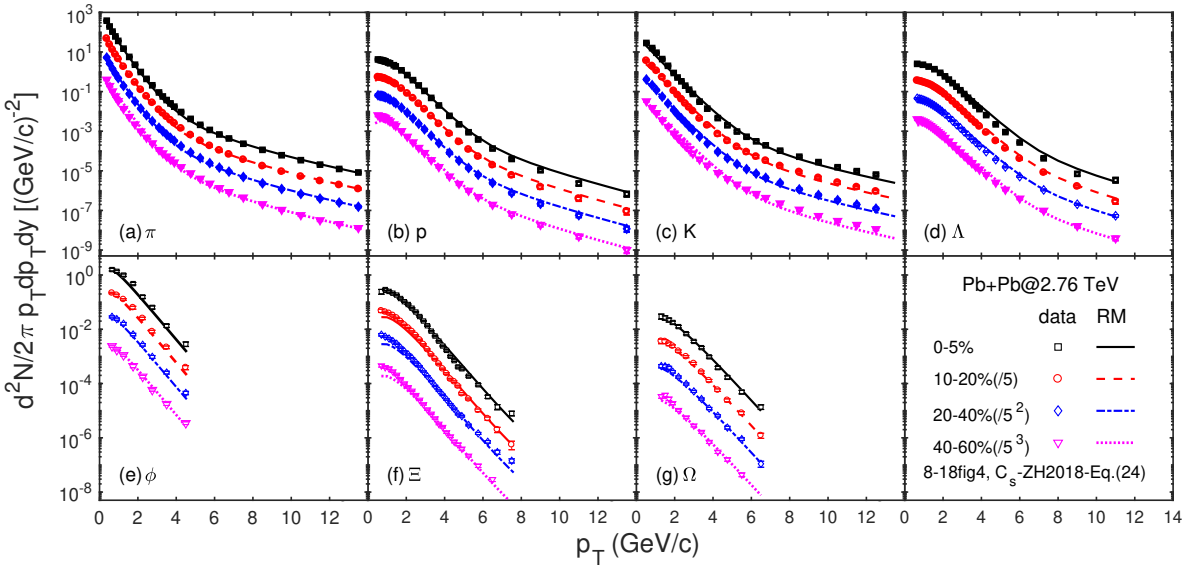

FIG. 3: (Color online) Transverse momentum spectra of pion (a), proton (b), kaon (c), Λ (d), ϕ (e), Ξ (f) and Ω (g) from the coalescence model at midrapidity in Pb+Pb collisions at $\sqrt{s_{NN}} = 2.76$ TeV for different centrality classes. Scale factors are applied for better visibility. The data are taken from Ref. [29] for pion, kaon and proton, Ref. [30] for ϕ, Ref. [31] for Λ and Ref. [32] for Ξ and Ω.

the theoretical curves fit the experimental data by just two parameters C and C_s in the centrality dependence of the thermal distribution. In each case, the TS, TTS and TSS components play crucial roles in uplifting the spectra in the intermediate region between low p_T where TT and TTT dominate and high p_T where SS and SSS dominate. That aspect of the p_T behavior has become the hallmark of the success of the recombination model, now extended to all centralities. Therefore, we can deduce that the recombination model is a sensible approach to describe the transverse momentum and centrality dependence of hadron production in the nuclear collisions.

V. SUMMARY

In this paper, we have studied seven identified hadron spectra in relativistic heavy ion collisions at LHC in the recombination model. Results from our calculations are found to nicely describe the centrality dependence of p_T spectra of π, p, K, Λ, ϕ, Ξ and Ω in Pb+Pb collisions at $\sqrt{s_{NN}} = 2.76$ and π, p and K at $\sqrt{s_{NN}} = 5.02$ TeV, respectively. We have also predicted the spectra of Λ, ϕ, Ξ and Ω at various centralities in Pb+Pb collisions $\sqrt{s_{NN}} = 5.02$ TeV, which can be compared with experimental measurements in the near future. The geometry and nuclear medium produced in heavy-ion collisions is complex, but the fact that our results from RM agree well with the measured data at all centralities and p_T for the seven identified hadrons supports the reliability of our description of the minijets and their shower partons.

The agreement between our model calculations and available data at LHC indicates that the recombination model, together with proper momentum degradation of hard or semihard partons, supports the picture that the centrality dependence of hadron production for the whole p_T region can described by the recombination of thermal and shower partons in relativistic heavy ion collisions at LHC. In this sense, we can conclude that the recombination model is one of the optimal approaches to describe the hadron production in high energy heavy-ion collisions.

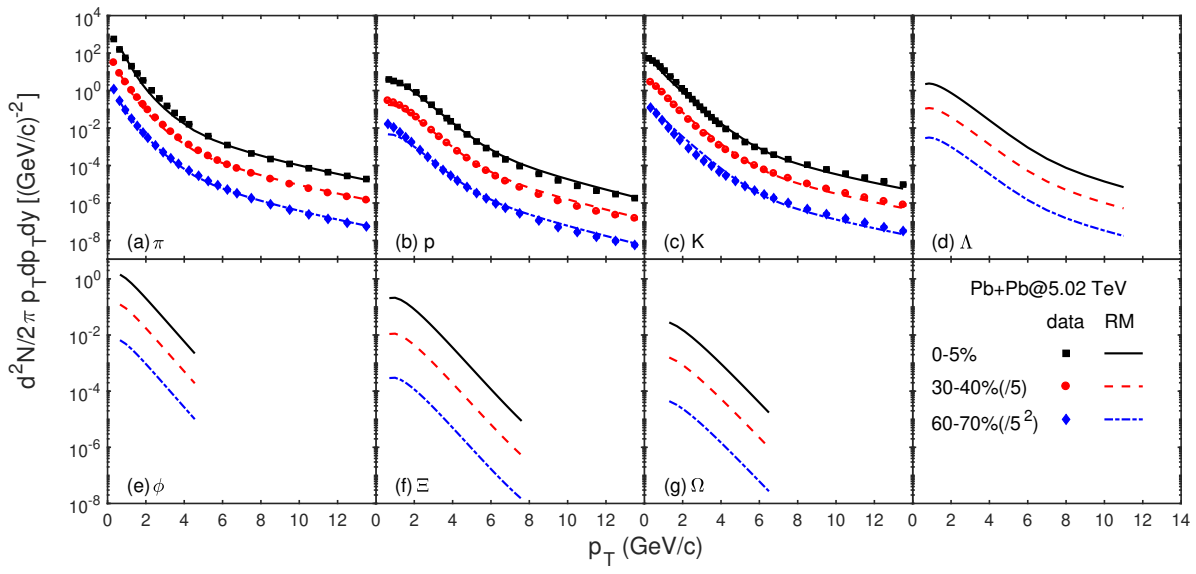

FIG. 4: (Color online) Transverse momentum spectra of pion (a), proton (b), kaon (c), Λ (d), ϕ (e), Ξ (f) and Ω (g) from the coalescence model at midrapidity for Pb+Pb collisions at $\sqrt{s_{NN}} = 5.02$ TeV and centralities of 0-5% (left panel), 30-40% (middle panel) and 60-70% (right panel). The experimental data for pion, kaon and proton are taken from Ref. [33].

Acknowledgements

This work was supported in part by the National Natural Science Foundation of China under Grant No. 11205106 and No. 11905120.

[1] P. F. Kolb and U. Heinz, in *Quark-Gluon Plasma 3*, edited by R. C. Hwa and X.-N. Wang (World Scientific, Singapore, 2004), p. 634.
[2] D. A. Teaney, in *Quark-Gluon Plasma 4*, edited by R. C. Hwa and X.-N. Wang (World Scientific, Singapore, 2010), p. 207.
[3] C. Gale, S. Jeon, and B. Schenke, Int. J. Mod. Phys. A **28**, 1340010 (2013).
[4] X.-F. Guo and X.-N. Wang, Phys. Rev. Lett. **85**, 3591 (2000); X.-N. Wang and X.-F. Guo, Nucl. Phys. A **696**, 788 (2001).
[5] Y. Mehtar-Tami, J. G. Milhano and K. Tywoniuk, Int. J. Mod. Phys. A **28**, 1340013 (2013).
[6] K. M. Burke *et al.* (JET Collaboration), Phys. Rev. C **90**, 014909 (2014).
[7] R. C. Hwa and C. B. Yang, Phys. Rev. C **67**, 034902 (2003).
[8] V. Greco, C. M. Ko, and P. Lévai, Phys. Rev. Lett. **90**, 202302 (2003); Phys. Rev. C **68**, 034904 (2003).
[9] R. J. Fries, B. Müller, C. Nonaka, and S. A. Bass, Phys. Rev. Lett. **90**, 202303 (2003); Phys. Rev. C **68**, 044902 (2003).
[10] Lilin Zhu and R. C. Hwa, Phys. Rev. C **88**, 044919 (2013).
[11] L. Zhu and R. C. Hwa, J. Phys. G **47**, 055102 (2020).
[12] Z. W. Lin, C. M. Ko, B. A. Li, B. Zhang and S. Pal, Phys. Rev. C **72**, 064901 (2005).
[13] X. N. Wang and M. Gyulassy, Phys. Rev. D **44**, 3501 (1991).
[14] L. Zhu, C. M. Ko and X. Yin, Phys. Rev. C **92**, 064911(2015).
[15] Y. He and Z. W. Lin, Phys. Rev. C **96**, 014910(2017) .
[16] B. A. Li and C. M. Ko, Phys. Rev. C **52**, 2037(1995).
[17] R. Mattiello, H. Sorge, H. Stoecker and W. Greiner, Phys. Rev. C **55**, 1443 (1997).
[18] L. W. Chen, C. M. Ko and B. A. Li, Phys. Rev. C **68**, 017601 (2003).
[19] L. W. Chen, C. M. Ko and B. A. Li, Nucl. Phys. A **729**, 809 (2003).
[20] C. M. Ko, T. Song, F. Li, V. Greco and S. Plumari, Nucl. Phys. A **928**, 234 (2014).
[21] C. Rappold *et al.* [HypHI Collaboration], Phys. Rev. C **88**, no. 4, 041001 (2013).
[22] W. Zhao, L. Zhu, H. Zheng, C. M. Ko and H. Song, Phys. Rev. C **98**, 054905 (2018).
[23] B. Abelev *et al.* [ALICE], Phys. Rev. C **88**, 044909 (2013).
[24] R. C. Hwa and C. B. Yang, Phys. Rev. C **70**, 024905 (2004).
[25] R. C. Hwa and Lilin Zhu, Phys. Rev. C **84**, 064914 (2011).
[26] R. C. Hwa and C. B. Yang, Phys. Rev. C **70**, 024904 (2004).
[27] R. C. Hwa and L. Zhu, Phys. Rev. C **97**, 054908 (2018).

[28] D. K. Srivastava, C. Gale, and R. J. Fries, Phys. Rev. C **67**, 034903 (2003).
[29] J. Adam *et al.* [ALICE], Phys. Rev. C **93**, 034913 (2016).
[30] B. B. Abelev *et al.* [ALICE], Phys. Rev. C **91**, 024609 (2015).
[31] B. B. Abelev *et al.* [ALICE], Phys. Rev. Lett. **111**, 222301 (2013).
[32] B. B. Abelev *et al.* [ALICE], Phys. Lett. B **728**, 216-227 (2014), [erratum: Phys. Lett. B **734**, 409-410 (2014)].
[33] S. Acharya *et al.* [ALICE], Phys. Rev. C **101**, 044907 (2020).
[34] S. Acharya *et al.* [ALICE], JHEP **1811**, 013 (2018).